Fish Physiol Biochem
https://doi.org/10.1007/s10695-021-00936-7

Gonadal lipidomics profile of an ovoviviparity teleost, black rockfish, during gonadal development

Jianshuang Li · Min Song · Haishen Wen · Ying Zhang · Yun Li · Likang Lyu · Xiaojie Wang · Xin Qi

Received: 15 October 2020 / Accepted: 10 February 2021

Abstract In order to study the variation of gonad lipidomics during reproductive cycle, black rockfish was employed as the research model in the present study. Using histology, lipidomics, and qPCR, the profile of gonad lipidomics and the expression levels of related genes during different developmental stages were detected and analyzed to show the potential regulatory network of lipid metabolism. Based on Ultra High-Performance Liquid Tandem Chromatography Quadrupole Time of Flight Mass Spectrometry (UHPLC-QTOFMS), four significant differential glycerophospholipid metabolic pathways including phosphatidylcholine (PC), phosphatidylethanolamine (PE), phosphatidylserine (PS), and phosphatidic acid (PA) were enriched by KEGG. Pathway-related enzyme-coding genes, including *phosphatidylserine decarboxylase* (*pisd*), *phosphatidylserine synthase* (*ptdss1*, *ptdss2*), and *phospholipase D* (*pld1*, *pld2*) were identified from the whole genome data and confirmed by cloning. The expression profiles of these genes were tested by qPCR in the tissues and gonads in developmental stages, and we found that *pisd*, *pld*, and *ptdss* genes were all downregulated through the developmental process in the brain of male, and the latter two genes were upregulated in the liver and testis at stage IV, which were the opposite trend observed in the female. Thus, our findings would be helpful in further understanding the substance metabolism and regulation during gonad development in ovoviviparity teleosts.

Keywords Black rockfish · Lipidomics · Glycerophospholipid lipidomics pathway · Gene expression

Introduction

Black rockfish (*Sebastes schlegelii*), which belongs to *Sebastes*, Scorpaenidae, has an ovoviviparous reproductive pattern and long-term sperm storage (Gao et al. 2017). Spermatogenesis starts in July, and the sperm matures from December to the following January. After sperm maturation, mating occurs through its modified urogenital papilla which emits spermatozoa into the female ovary. The sperm are stored afterwards in the ovary during the early vitellogenesis period and under the ovigerous lamellae epithelium during the late period (Mori et al. 2011). While in female, vitellogenesis starts in November and oocytes mature from late March to early April. After the activation of sperm and fertilization in April, the female starts pregnancy, which lasts for approximately 37 days, and parturition occurs in May (Kawaguchi et al. 2010). The reproductive strategy of asynchronous gonadal development may develop from

J. Li · H. Wen · Y. Zhang · Y. Li · L. Lyu · X. Wang · X. Qi (✉)
Key Laboratory of Mariculture, Ministry of Education, Ocean University of China, Qingdao, People's Republic of China
e-mail: qx@ouc.edu.cn

M. Song
College of Animal Science, Inner Mongolia Agricultural University, Hohhot, Inner Mongolia, People's Republic of China

Published online: 10 March 2021

adaptive evolution. However, the nutritional requirements, lipid metabolism, and related regulation processes during the gonadal development process in both sexes remain unclear. Taken together, the different seasonal effects on both gonad development and nutritional requirements in different sexes are still unknown.

Oocyte quality is one of the key limitations of female fertility. Lipid metabolism, an important indicator of oocyte quality (Paulini et al. 2014; Warzych et al. 2017), is considered as the crucial source of energy for oocyte growth, maturation, fertilization, and embryo development (Hashemi and Goodman 2015; Marei et al. 2012; Paczkowski et al. 2014). During the whole vitellogenesis stage, lipids are transferred by follicular cells into the oocyte where lipids are stored (Warzych et al. 2017). On the other hand, nutritional storage affects not only the fecundity of female fish but also the quality of sperm (Huang et al. 2010). Lipids are important for the activation of membrane enzymes, motility, and sperm capacitation (Aloia 1983). Additionally, the phospholipids play important roles in the membrane stability and stress resistance of sperm and protect spermatozoa from osmotic and cold shock (Simpson et al. 1986). During the reproductive cycle, lipids transform to provide suitable nutrition for gonadal development, indicating differences in energy requirements and utilization between the ovary and testis during different developmental stages (Huang et al. 2010; Songlin et al. 2018).

Phospholipids (PLs), especially glycerophospholipids (GPs), are the major components of all biological membranes and have important structural and functional roles (Hu et al. 2009; Küllenberg et al. 2012; Mürke et al. 2016; Nicolson and Ash 2017). Glycerophospholipids are composed of phospholipid acids and substituted groups linked to phosphoric acid, and they can be divided into many categories according to the different substituted groups, with most important ones including phosphatidylcholine (PC), phosphatidyl ethanolamine (PE), phosphatidylserine (PS), phosphatidylinositol (PI), phosphatidic acid (PA), phosphatidylglycerol (PG), and cardiolipin (CL) (Calzada et al. 2016; Goldfine 1982).

PC is the main energy material in the gonad of fish and plays an important role in germ cell differentiation, embryonic development, and survival of larval and juvenile fish. PE, the second most abundant phospholipid, serves to enhance the liquid crystal properties of membranes (Wiegand 1996). PS, used to identify apoptosis, is abundant in apoptotic cells to induce phagocytosis of macrophages (Blankenberg et al. 1998; Rücker-Martin et al. 1999; Zwaal and Schroit 1997). PA is the simplest glycerophospholipid and acts as a lipid second messenger that involved in various intracellular events (English et al. 1996; Exton 1994; Lee et al. 1998).

PC is synthesized by two distinct pathways including the methylation pathway or the CDP-choline pathway (Aktas et al. 2010; Geiger et al. 2013; Sohlenkamp et al. 2003). The synthesis of PC is limited by phosphocholine cytidylyltransferase (CCT), which is an amphitropic enzyme that regulates PC homeostasis (Taneva et al. 2019). PE is synthesized by two major biosynthetic pathways: the CDP-ethanolamine pathway and the PS decarboxylase pathway where PS is decarboxylated to PE and then methylated to form PC (Borkenhagen et al. 1961; Dennis 2003; Vance 2015; Vance and Tasseva 2013). In mammals, Ptdss1 and Ptdss2 synthesize PS with PC and PE as substrates, respectively. The synthesis process is rate limited by Ptdss1 but not Ptdss2 (Stone and Vance 1999). *ptdss1* is widely expressed in all tissues and enriched in the brain and skeletal muscle of mice (Sturbois-Balcerzak et al. 2001). In contrast, PS is less synthesized by Ptdss2 in other cell types with predominantly expressed in the testis (Bergo et al. 2002; Sturbois-Balcerzak et al. 2001). A lack of Ptdss2 can cause incomplete testis development in mice, leading to infertility (Bergo et al. 2002). PA can be formed from other phospholipids by the action of Pld (Buckland and Wilton 2000).

To further understand the lipid synthesis process in asynchronous development during oogenesis and spermatogenesis of an ovoviviparity teleost, LC-MS/MS analyses were employed to detect the variation in phospholipids during both processes. Several important genes encoding lipid metabolism-related enzymes were also identified and examined during gonadal development. These novel findings demonstrate a similar lipid requirement in different sexes of ovoviviparity fish, although the development time course varies. Our results also confirmed the conservation of the glycerophospholipid lipidomics pathway from teleost to mammals.

Materials and methods

Ethics statement

All animal experiments were conducted in accordance with the guidelines and approval of the respective

Animal Research and Ethics Committees of the Ocean University of China.

Animals and sample collection

From October 2016 to June 2017, 36 male and female black rockfish were purchased every month from a local fish market in Qingdao, China, and black rockfish were obtained from cage aquaculture (Dalian, Liaoning, China). Without temporary rearing, all fish were anesthetized with tricaine methanesulfonate (MS-222, 0.1 g/L) before sample collection. Tissues, including heart, liver, spleen, kidney, head kidney, stomach, intestine, muscle, brain, gill, gonad, pituitary, skin, and adipose tissue, were collected and immediately frozen in liquid nitrogen and stored at −80 °C for further detection. Part of the gonad was used for lipidomics experiments and gene expression detection. Other parts of the gonad were fixed in Bouin's solution for developing stage confirmation. Six biological replicates of each developmental stage were used for experimental research.

Developing stage confirmation

Fixed gonads were dehydrated in a 30–100% ethanol series, transparent by xylene, embedded in paraffin wax, and sliced into 6–8-μm-thick paraffin sections by microtome (Leica, Wetzler, Germany), followed by the hematoxylin-eosin staining. The slices were then photographed by light microscopy to confirm the developmental stages (Olympus, Tokyo, Japan).

Lipidomics method

The samples added 0.68 ml extraction liquid (V_{MTBE}:$V_{methanol}$:V_{H2O} = 10:2:5) were homogenized in ball mill for 4 min at 45 Hz, ultra-sounded for 5 min on ice, incubated at −20 °C for 1 h, and centrifuged for 15 min at 12000 rpm, 4 °C. Then, 0.35 ml of the upper MTBE phase was transferred to a new EP tube and evaporated to dry and reconstituted with 100 μl of 1:1 v/v DCM: MeOH. The 70 μl supernatant was transferred into a fresh 2 ml LC/MS glass vial, 10 μl from each sample was pooled as QC samples, and 70 μl supernatant was collected for UHPLC-QTOF-MS analysis.

LC-MS/MS analyses were performed using a UHPLC system (1290, Agilent Technologies) with a Phenomen Kinetex 1.7u C18 100A Column (100 × 2.1 mm), coupled to a Triple TOF 6600 (Q-TOF, AB Sciex). The mobile phase consisted of A: 10 mM $HCOONH_4$ + 40% H_2O + 60% CAN; B: 10 mM $HCOONH_4$ + 10% ACN + 90% IPA.

The Triple TOF mass spectrometer was used because of its ability to acquire MS/MS spectra on an information-dependent basis (IDB) during an LC/MS experiment. In this mode, the acquisition software (Analyst TF 1.7, AB Sciex) continuously evaluated the full-scan survey MS data as it collected and triggered the acquisition of MS/MS spectra depending on preselected criteria. In each cycle, 12 precursor ions with intensities greater than 100 were chosen for fragmentation at a collision energy (CE) of 45 ± 25 V (15 MS/MS events with a product ion accumulation time of 50 msec each).

Gene sequence confirmation and phylogenetic tree

The sequences of lipid metabolism-related genes were obtained from the transcriptome sequencing data with accession number SRR4409372 and were confirmed by gene cloning. The gene sequences were submitted to the NCBI database (on March 14, 2020) under the following accession numbers: *ptdss1* (MT188672), *ptdss2* (MT188673), *pld1* (MT188674), *pld2* (MT188675), and *pisd* (MT188676). Phylogenetic analyses were carried out using MEGA 7.0 and the neighbor-joining (NJ) method.

Gene expression detection with q-PCR

Total RNA was extracted from black rockfish tissues using TRIzol® reagent (Invitrogen, USA) according to the manufacturer's protocols, and its concentration and purity were measured by a biophotometer (OSTC, China) and agarose gel electrophoresis, respectively. One microgram of total RNA was used as a template for reverse transcription using PrimeScript™ RT reagent Kit with gDNA Eraser (Perfect Real Time) (Takara, Japan) according to the manufacturer's protocols.

All primers used in the present study were listed in Table 1. The qPCR reaction mixture (20 μl) contained 10 μl of SYBR® Premix Ex Taq (×2), 2 μl cDNA template, 0.4 μl of both primers, 0.4 μl of ROX Reference Dye (×50), and 6.8 μl of RNase-free water. The qPCR procedure was performed as follows: predenaturation at 95 °C for 30 s, 40 cycles of denaturation at 95 °C for 5 s, annealing temperature for 30 s, and a final extension at 72 °C for 2 min. The results of the gene melting curve were single peaks, which confirmed

Table 1 Primer sequences for mRNA expression analysis

Genes	Primers sequence (5′ to 3′)
18*s*	F: CCTGAGAAACGGCTACCACAT
	R: CCAATTACAGGGCCTCGAAAG
pld1	F: AGCAACGGGAAAGGAATC
	R: TGTGCCTGTCTATGAAGTCG
pld2	F: CCTTCTTCCCAAGTCTCA
	R: TTCGGTTCACGATTGC
ptdss1	F: AAAGACATCCACTCCACCAC
	R: CCAAACAGGCACAGGAAT
ptdss2	F: GTGACGCAAGCCAAAG
	R: CATCCCAGGAAGTGAGC
pisd	F: CCAGGTGACTACCACTGTTTC
	R: CGAAGTAAACCCTGATGGAG

the specificity of the PCR results. At the same time, 18s RNA was used as the internal reference to normalize the qPCR veracity, and the samples were run in triplicate (Ma et al. 2013). qPCR was performed by the StepOnePlus™ Real-Time PCR system (Applied Biosystems, America), and the $2^{-\Delta\Delta CT}$ method was used to analyze the expression level of genes (Livak and Schmittgen, 2001).

Statistical analysis

All data were expressed as the mean values ± S.E.M. Data analyses were processed by normal distribution and homogeneity test of variances before performed by one-way ANOVA, and then Duncan's multiple range test was also used, and significance was considered at $P < 0.05$. All statistics were performed using SPSS 17.0 (SPSS, Chicago, IL, USA).

Results

The histology of gonads in different developmental stages

To confirm the developmental stages of the samples in the lipidomics test, the histology of the samples was examined first. The testis samples were identified at stage III (early spermatogenesis), stage IV (late spermatogenesis), and stage V (regressed). In the early spermatogenesis stage (Fig. 1a), spermatozoa matured gradually in spermatogenic cysts and then filled the lobular lumen and vas deferens continuously in the late spermatogenesis stage (Fig. 1b). When spermatozoa were expelled out of the body, the remaining sperm degenerated and died, and then the testis entered the regressed stage (Fig. 1c). The ovarian samples were identified mainly at stage II (regeneration), stage IV (vitellogenesis), and stage V (maturation). As shown in Fig. 1d, oocytes were mainly in the second phase with clear nucleus. With the increasing volume of oocytes, yolk granules gradually became clear, and oocytes mainly developed to the fourth phase (Fig. 1e). When yolk granules filled the oocyte and began to liquefy, and the germinal vesicle migrated, the ovary entered stage V (Fig. 1f).

Differential metabolite responses during testis development

Sample quality control was shown in Figs S1 to S3, and no overfitting phenomenon was found in the model construction. Based on the criteria, VIP>1.0 and $P<0.05$ in the OPLS-DA model, differential metabolites were chosen and visualized in the form of volcano maps (Figs. 2 and 3). To determine the variation characteristics of the same metabolite between different stages, a heatmap of the hierarchical clustering analysis was applied to the differential metabolites with significant up- and downregulation in the above results (Figs. 2 and 3). Compared to stage III, 147 metabolites were upregulated and 35 were downregulated in positive ion mode, and 78 were upregulated and 26 were downregulated in negative ion mode in stage IV, and 117 were upregulated and 36 were downregulated in positive mode, and 108 were upregulated and 55 were downregulated in negative ion modes of stage V (Fig. 2 and 3). Among the significantly varied metabolites, phospholipids were the major type, including phosphatidyl ethanolamine (PE), phosphatidylcholine (PC), phosphatidylserine (PS), phosphatidic acid (PA), phosphatidylglycerols (PG), and phosphatidylinositols (PI). The quantity of other metabolites, including carnitine, sphingosine, triglyceride, cholesterol, and ceramide (Cer), was limited.

Lipidomics pathway analysis of different metabolites in male fish

Lipidomics pathways related to gonadal development of the male black rockfish were determined by matching differential metabolites that had significant differences with the HMDB (Human Metabolome Database), PubChem, KEGG (Kyoto Encyclopedia of Genes and

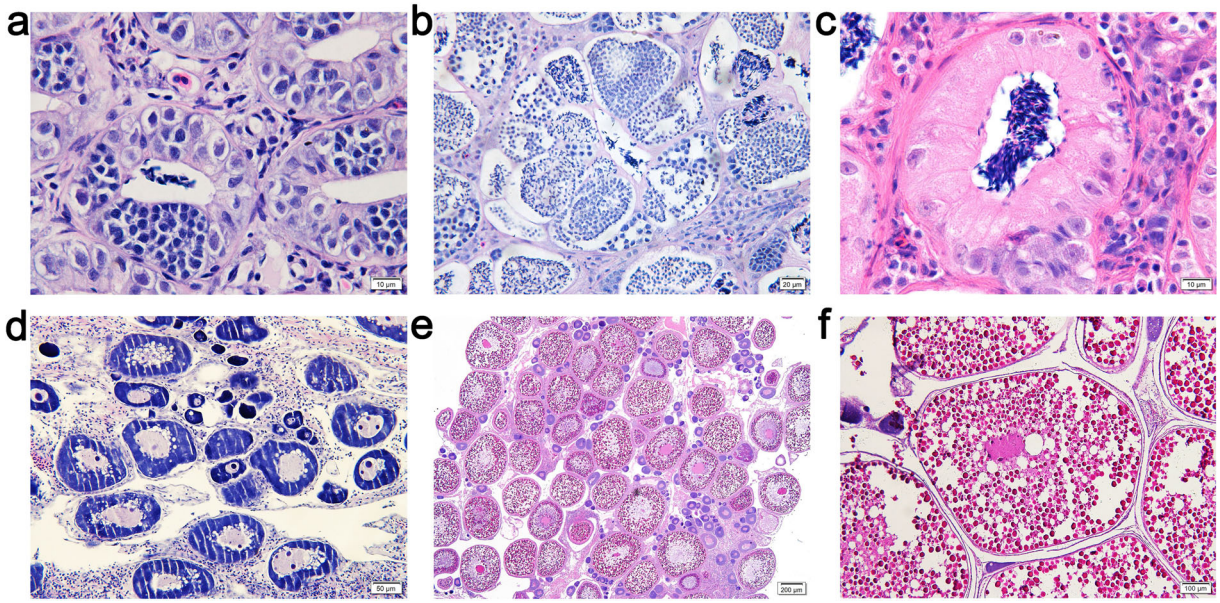

Fig. 1 The histologic results of the gonad of black rockfish. **a**–**c** shows the different stage of testis, and they were in the early spermatogenesis and late spermatogenesis and regressed, respectively. **d**–**f** shows the different stages of ovaries, and they were in the regeneration, vitellogenesis, and maturation, respectively

Genomes), and other databases. By annotating the lipidomics pathways by KEGG, 24 pathways in positive and 8 in negative ion mode were obtained between stages IV and III, while 24 and 12 pathways in positive and negative ion mode were obtained between stages IV and V.

To identify the lipidomics pathways that showed the highest correlation with the differential metabolites, the enriched pathways were shown in Fig. 4. Eight lipidomics pathways were enriched between stages IV and III, and seven were enriched between stages V and IV. Six lipidomics pathways, including glycerophospholipid metabolism, linoleic acid metabolism, alpha-linolenic acid metabolism, glycosylphosphatidylinositol (GPI)-anchor biosynthesis, glycerolipid metabolism, and arachidonic acid metabolism, were shared in the testis development process. Among these pathways, the glycerophospholipid lipidomics pathway showed the most significant variation. The amount of lipidomics of PA, PC, PE, and PS varied the most significantly (Tables 2 and 3).

Differential metabolite responses during ovary development

Sample quality control was shown in Figs S4 to S6, and no overfitting phenomenon was found in the model construction. Differentially expressed metabolites' heatmap of hierarchical clustering analysis for ovary development was shown in Figs. 5 and 6. Between stages IV and II, 40 metabolites were upregulated and 54 were downregulated in positive ion mode, and 70 were upregulated and 22 were downregulated in negative ion mode. Between stages V and IV, 28 were upregulated and 22 were downregulated in positive ion mode, and 49 were upregulated and 22 were downregulated in negative ion mode (Figs. 5 and 6).

Lipidomics pathway analysis of differential metabolites in female fish

Similar to males, six lipidomics pathways were enriched between both stages IV and II and stages V and IV in females, including glycerophospholipid metabolism, linoleic acid metabolism, alpha-linolenic acid metabolism, glycosyl-phosphatidylinositol (GPI)-anchor biosynthesis, glycerolipid metabolism, and arachidonic acid metabolism (Fig. 7, Tables 4 and 5). The glycerophospholipid lipidomics pathway still showed the most significant variation.

Glycerophospholipid synthesis-related gene expression during gonadal development

According to the lipidomics results, four metabolites were enriched in the present study. To further

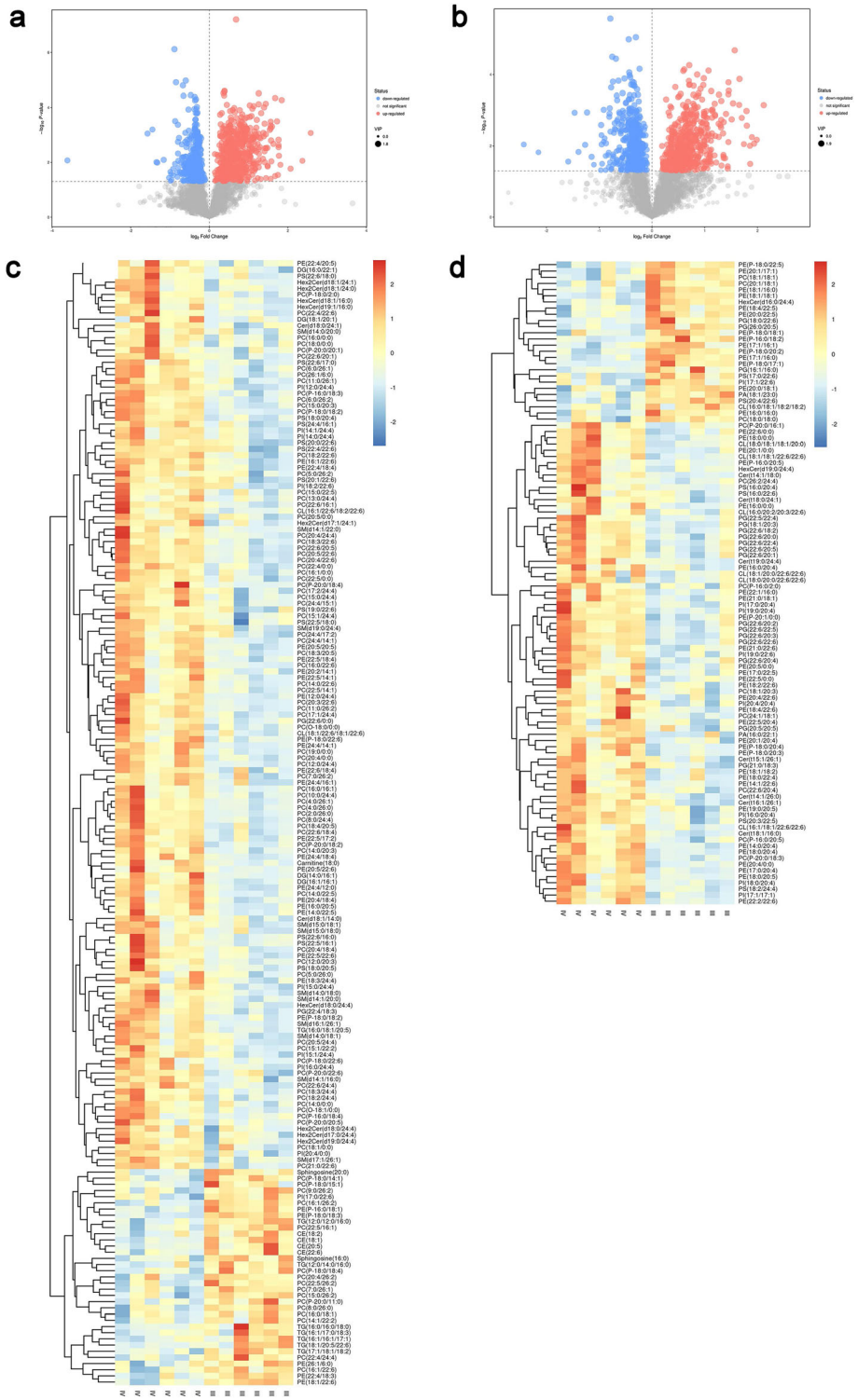

Fig. 2 The volcano plot (**a**, **b**) and the heatmap of hierarchical clustering analysis (**c**, **d**) were applied to differential metabolites of testis between stage IV and III. **a**, **b** The volcano plot between stage IV and III in positive and negative ion mode, respectively. The different color plots represent the variety of metabolites; the blue, red, and gray plots represent down, up, and no regulation, respectively. **c**, **d** The differential metabolites between stages IV and III in positive and negative ion mode, respectively

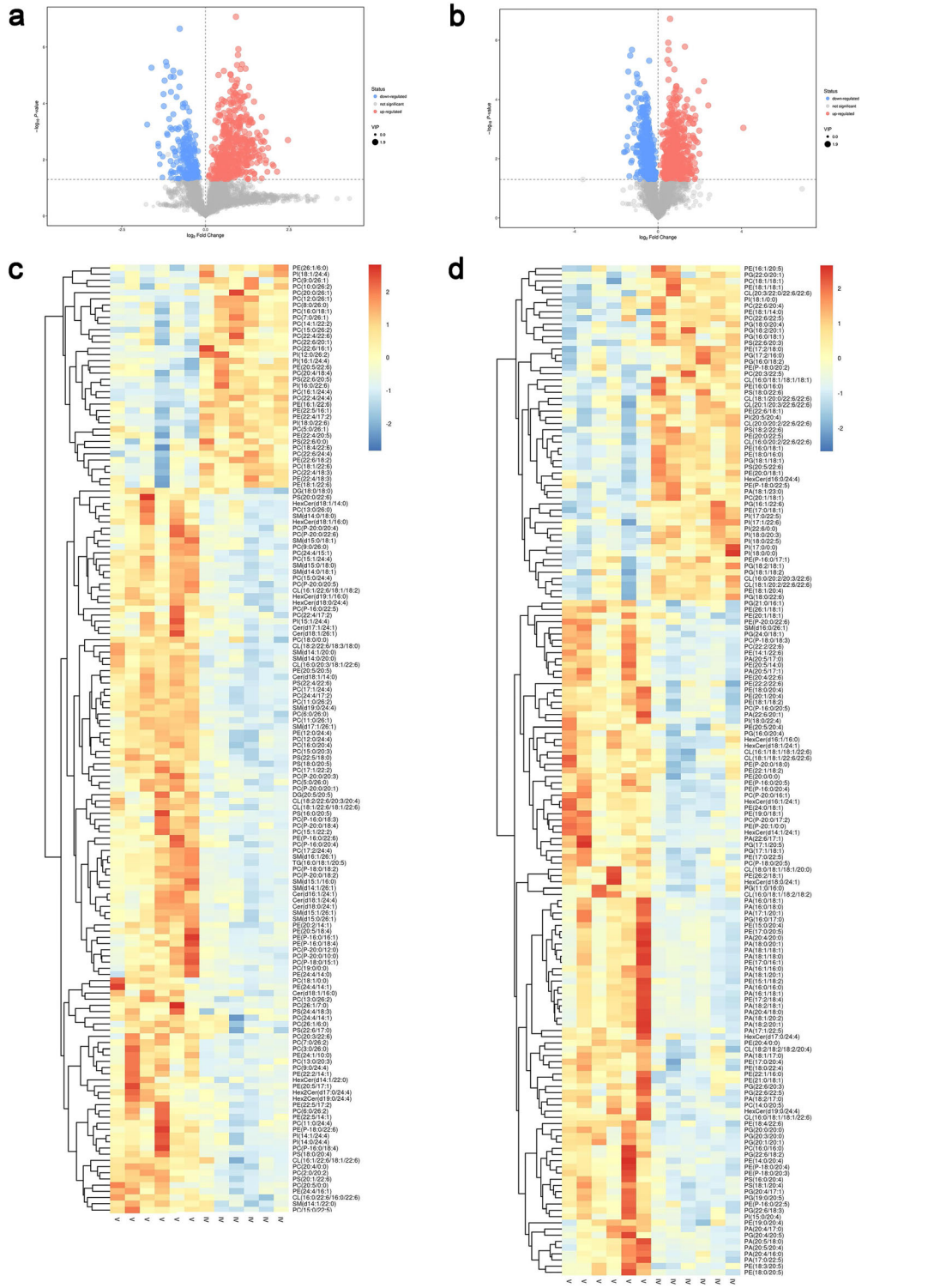

Fig. 3 The volcano plot (**a**, **b**) and the heatmap of hierarchical clustering analysis (**c**, **d**) were applied to differential metabolites of testis between stages V and IV. **a**, **b** The volcano plot between stages V and IV in positive and negative ion mode, respectively. The different color plots represent the variety of metabolites; the blue, red, and gray plots represent down, up, and no regulation, respectively. **c**, **d** The differential metabolites between stages V and IV in positive and negative ion mode, respectively

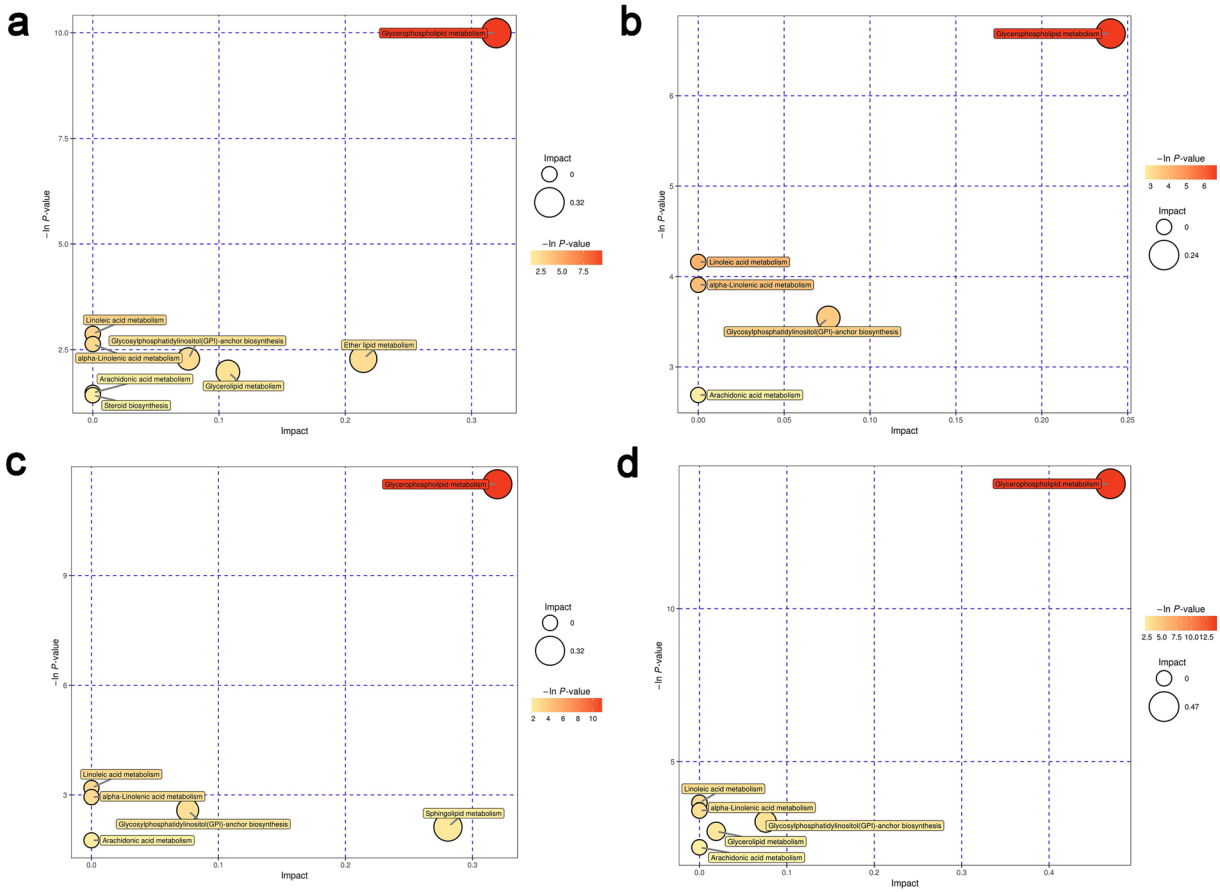

Fig. 4 The bubble plot of pathway enrichment was based on the differential metabolites through the use of KEGG database. **a**, **b**, **c**, and **d** represent the pathway enrichment between stages IV and III and stages V and IV in positive and negative ion mode, respectively. The bigger the bubble was, the darker the color was, and the smaller the *P* value was, indicating that the higher the influence factors and the correlation of the pathways were. And the most significant pathway was glycerophospholipid metabolic pathway in all modes

verify lipid biosynthesis, five genes encoding key enzymes that participate in biological processes were chosen as targets. By cloning and constructing the phylogenetic analysis (Fig. S7), the sequences of genes, including *pld1*, *pld2*, *ptdss1*, *ptdss2*, and *pisd*, were confirmed. The tissue distribution of these genes was shown in Fig. S8. Both *pld* and *ptdss1* showed the highest expression in the brain, while *pisd* was mainly expressed in the liver and showed high expression in the brain. *ptdss2* was also highly expressed in the gonad.

According to the tissue distribution results, the brain, liver, and gonad were chosen as the target organs for the testing of gene expression. In males (Fig. 8), both *pld* and *ptdss* were downregulated through the development process in the brain and upregulated in the liver and testis at stage IV but downregulated in stage V. The expression of *pisd* decreased significantly during spermatogenesis. In females (Fig. 9), the expression of *pld*, *ptdss*, and *pisd* was enhanced significantly in the brain but decreased in the ovary during vitellogenesis.

Discussion

Lipids play a crucial role in the development of oocytes and embryos and not only act as substrates for energy metabolism but also as structural components in membrane biogenesis (Huang et al. 2010). In the present study, we determined that during the whole reproductive period, lipid levels of gonads in both sexes varied significantly, and the main differential lipidomics pathways were focused on glycerophospholipid metabolism, including PC, PE, PS, PG, and PI.

Table 2 Related metabolic pathways and corresponding difference metabolites between stages IV and III of male black rockfish

Pathway	Hits	Metabolites	Trend	Ion mode	-ln(p)	Impact
Glycerophospholipid metabolism	4	Phosphatidylethanolamine Phosphatidylcholine	↑ ↑	Positive	9.9915	0.31961
		LysoPC (18:1(9Z)) PS (16:0/16:0)	↑ ↑	Negative	6.685	0.24006
Linoleic acid metabolism	1	Phosphatidylcholine	↑	Positive	2.8783	0
				Negative	4.1596	0
Alpha-linolenic acid metabolism	1	Phosphatidylcholine	↑	Positive	2.6344	0
				Negative	3.9098	0
Glycosylphosphatidylinositol (GPI)-anchor biosynthesis	1	Phosphatidylethanolamine	↑	Positive	2.2816	0.07576
				Negative	3.5451	0.07576
Ether lipid metabolism	1	LysoPC (O-18:0)	↑	Positive	2.2816	0.21429
Glycerolipid metabolism	1	Triacylglycerol	↓	Positive	1.9747	0.10704
Arachidonic acid metabolism	1	Phosphatidylcholine	↑	Positive	1.4789	0
				Negative	2.6896	0
Steroid biosynthesis	1	CE (16:1(9Z))	↓	Positive	1.4236	0

In males, the spermatozoa have a unique lipid structure that transforms to adopt physiological changes in the body in the process of maturation (Castellini et al. 2006). Phospholipids play an important role in the acrosomal reaction, membrane enzymes activation, sperm motor activity, and capacitation (Hinkovska-Galcheva et al. 1989). The highest content of lipids in marine fish sperm is PC (Drokin 1993), which has a strong affinity with the cell membrane to protect sperm from cold shock (Evans and Setchell 1978; Simpson et al. 1986). In the present study, the increase in PE and PC in males could ensure the vitality and quality of sperm and avoid the impact of cold on sperm during the cold winter. On the other hand, PS is an intermediate product of lipid metabolism that is involved in signal regulation of growth and development, and it was maintained at a high level at the early stage of testis development and thus could provide resources for the synthesis of other lipids. However, the increase in PS at sperm maturation is possibly due to the localization of PS to the surface of

Table 3 Related metabolic pathways and corresponding difference metabolites between stage V and IV of male black rockfish

Pathway	Hits	Metabolites	Trend	Ion mode	-ln(p)	Impact
Glycerophospholipid metabolism	4	Phosphatidylethanolamine Phosphatidylcholine	↑ ↑	Positive	11.499	0.31961
		PS (16:0/16:0) PA (16:0/16:0)	↓ ↑	Negative	14.094	0.47018
Linoleic acid metabolism	1	Phosphatidylcholine	↑	Positive	3.19	0
				Negative	3.6533	0
Alpha-linolenic acid metabolism	1	Phosphatidylcholine	↑	Positive	2.9439	0
				Negative	3.405	0
Glycosylphosphatidylinositol (GPI)-anchor biosynthesis	1	Phosphatidylethanolamine	↑	Positive	2.5867	0.07576
				Negative	3.0432	0.07576
Sphingolipid metabolism	1	Ceramide	↑	Positive	2.1279	0.2807
Glycerolipid metabolism	1	PA (16:0/16:0)	↑	Negative	2.7253	0.0192
Arachidonic acid metabolism	1	Phosphatidylcholine	↑	Positive	1.7644	0
				Negative	2.2011	0

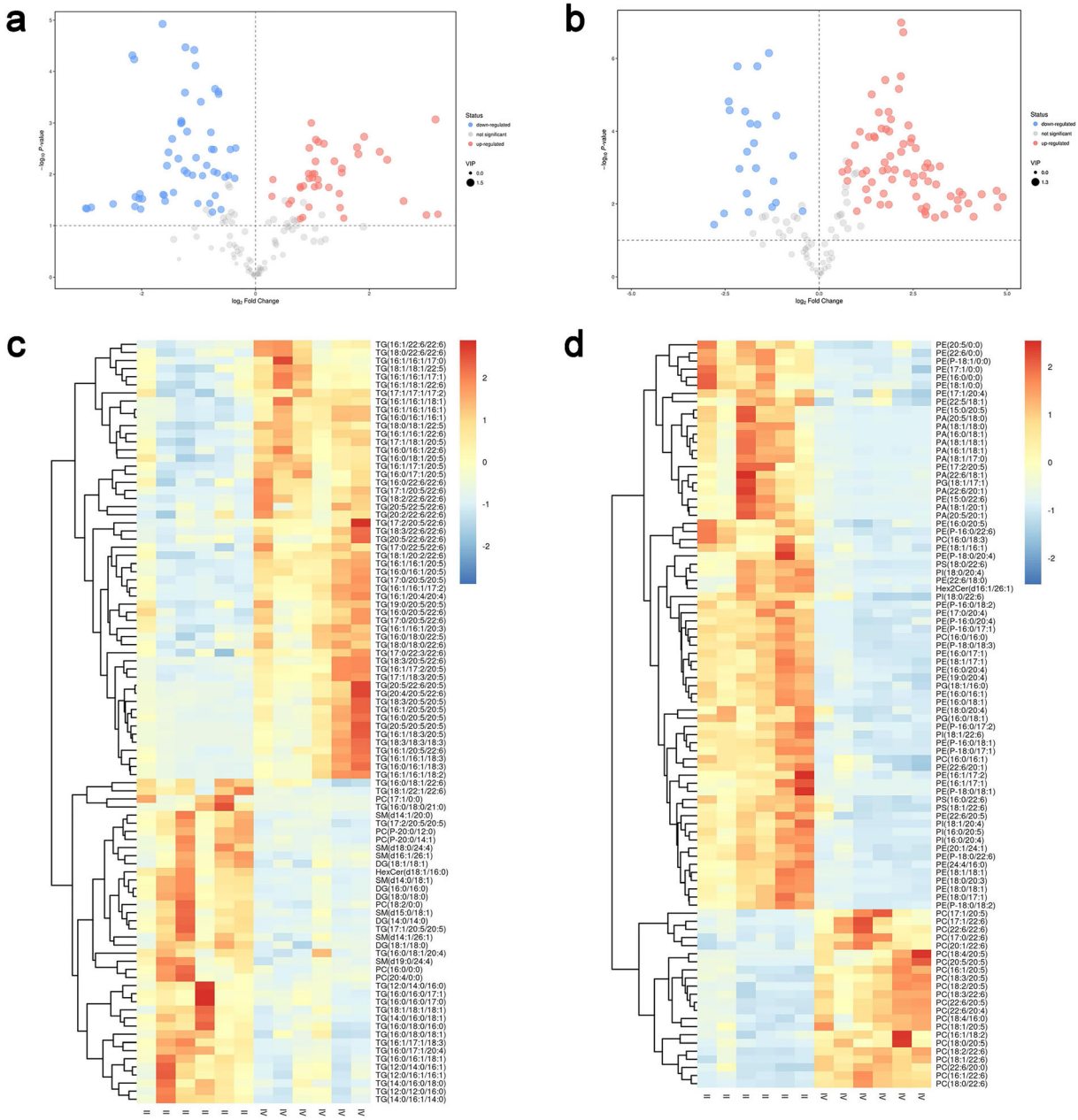

Fig. 5 The volcano plot (**a**, **b**) and the heatmap of hierarchical clustering analysis (**c**, **d**) were applied to differential metabolites of ovaries between stages IV and II. **a**, **b** The volcano plot between stages IV and II in positive and negative ion mode, respectively. The different color plots represent the variety of metabolites; the blue, red, and gray plots represent down, up, and no regulation, respectively. **c**, **d** The differential metabolites between stages IV and II in positive and negative ion mode, respectively

sperm during development (Vance and Tasseva 2013). As a precursor of other lipids, PA always continues to increase during testis development to ensure the synthesis of other lipids.

The fertility of teleost is usually represented by the number of eggs carried by female fish, and nutritional conditions are the key factor affecting fecundity. The nutrients of teleost are usually stored in oil pellets and yolk in the form of PC and PE (Salze et al. 2010; Wiegand 1996); therefore, unsaturated fatty acids (UFAs) increase significantly in the middle and late stages of yolk development (Roustaian et al. 1999;

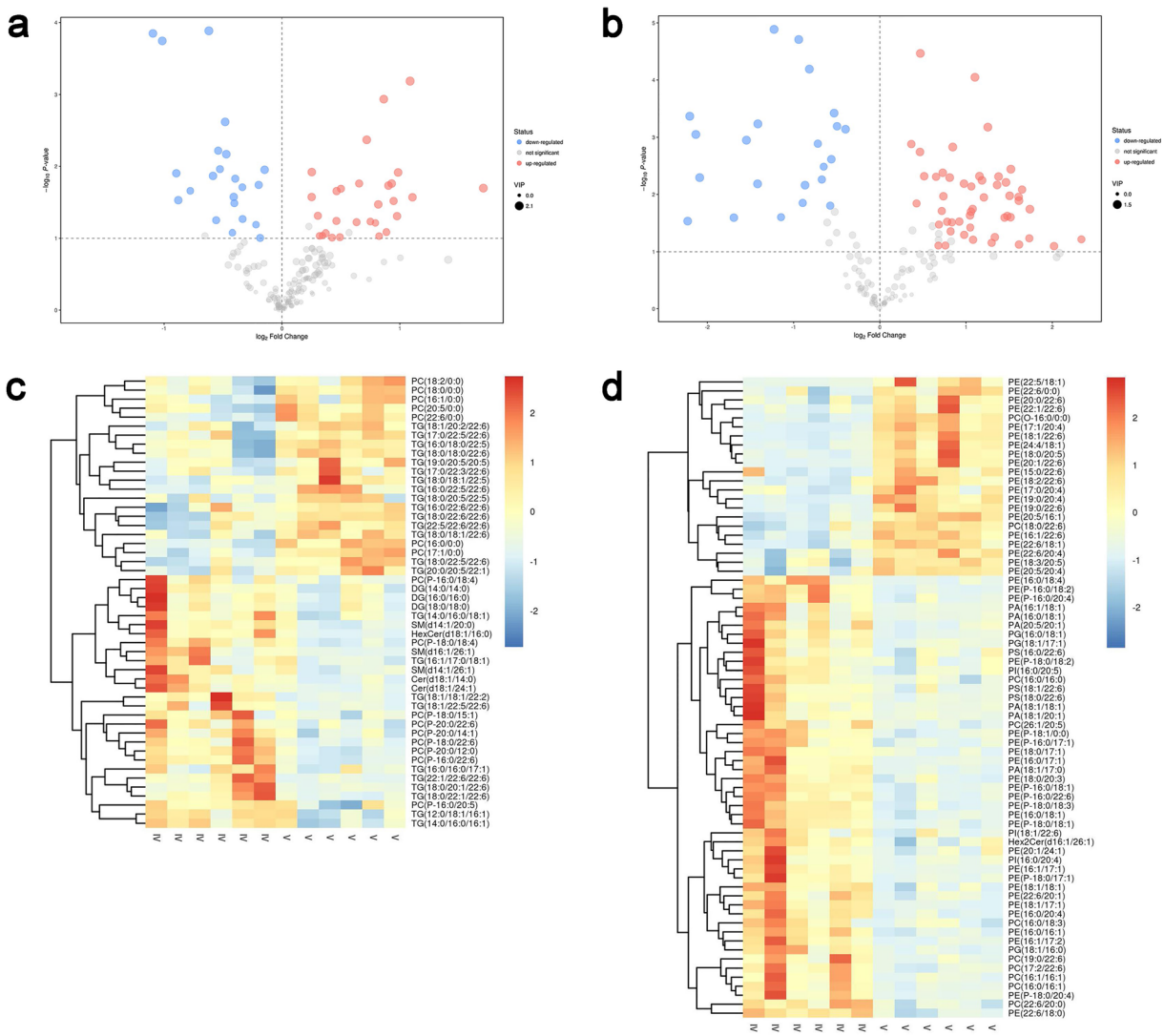

Fig. 6 The volcano plot (**a**, **b**) and the heatmap of hierarchical clustering analysis (**c**, **d**) were applied to differential metabolites of ovaries between stages V and IV. **a**, **b** The volcano plot between stages V and IV in positive and negative ion mode, respectively. The different color plots represent the variety of metabolites; the blue, red, and gray plots represent down, up, and no regulation, respectively. **c**, **d** The differential metabolites between stages V and IV in positive and negative ion mode, respectively

Wouters et al. 2001). The oocytes of black rockfish started to accumulate nutrients at stage II as observed from the histology results. Similarly, PC, which acts as a source of endogenous nutrients in oocytes and fertilized eggs, increased at stage IV compared with stage II. However, the PE level decreased significantly in the maturation stage. During the maturation process, yolk granules begin to fuse, and some PE is converted into arachidonic acid, which further stimulates the synthesis of steroids in ovaries and promotes the final maturation of oocytes. Indeed, the main nutrient of female black rockfish in the breeding period was PC, and most PS was converted into PC by phospholipid synthase through self-regulation, thus providing sufficient nutrients for the development of oocytes and fertilized eggs. Consistent with previous results in skipjack tuna (Hiratsuka et al. 2004), the level of glycerol phospholipids of ovaries was significantly reduced at stage V. At final maturation, the oocytes are fully developed, and the lipids in the ovaries are rapidly hydrolyzed for energy (Toyomizu et al. 1977). Oocytes are ready for sperm activation and fusion between sperm and oocytes,

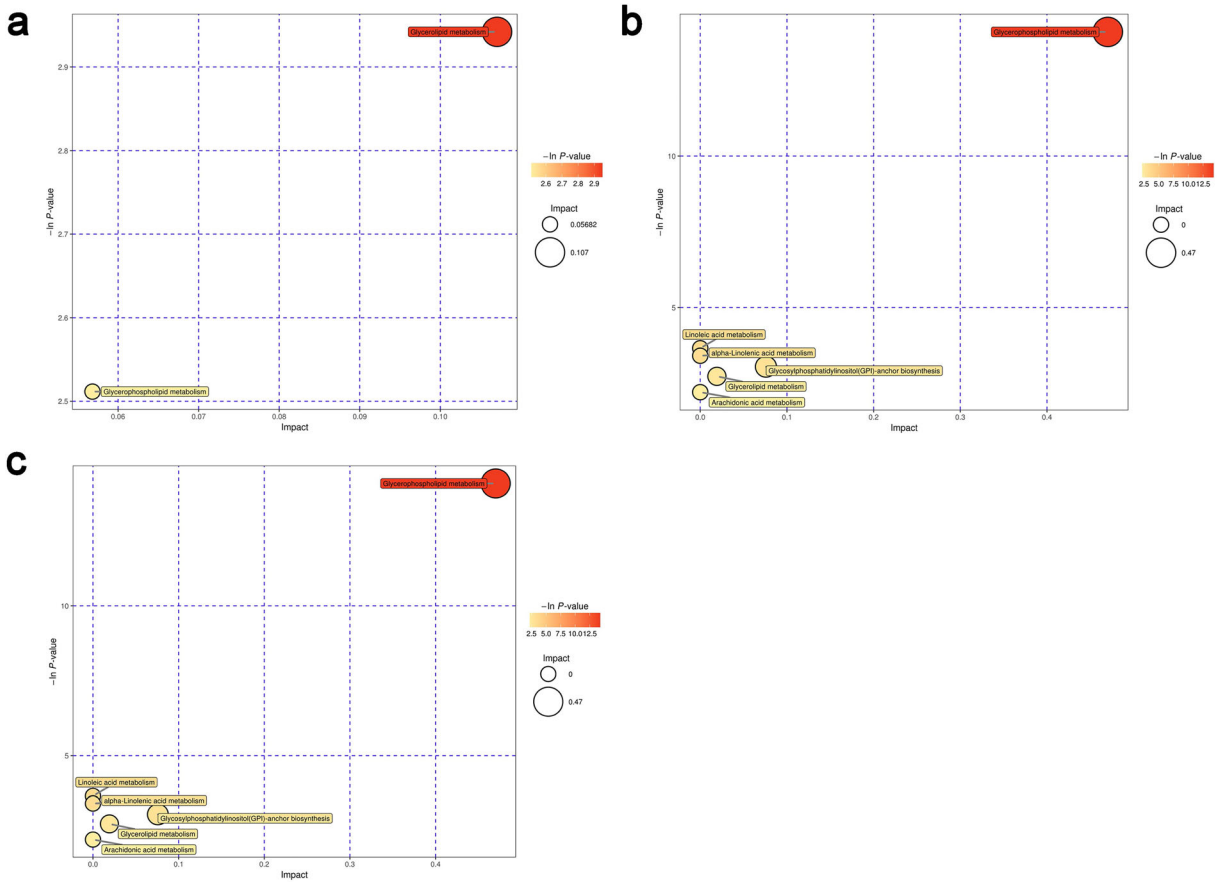

Fig. 7 The bubble plot of pathway enrichment was based on the differential metabolites through the use of KEGG database. **a**, **b** The pathway enrichment between stages IV and II in positive and negative ion mode, respectively. The bigger the bubble was, the darker the color was, and the smaller the *P* value was, indicating that the higher the influence factors and the correlation of the pathways were. **c** The pathway enrichment between groups V and IV in negative ion mode. And the most significant pathway was glycerophospholipid metabolic pathway in all modes

in which PE is methylated to form PC that is consumed to produce energy so that the ratio of PC to PE is reduced to a normal level (Tocher et al. 2008). In addition, a shift occurs between different fatty acid classes

Table 4 Related metabolic pathways and corresponding difference metabolites between stages V and II of female black rockfish

Pathway	Hits	Metabolites	Trend	Ion mode	-ln(p)	Impact
Glycerophospholipid metabolism	4	Phosphatidylethanolamine Phosphatidylcholine	↓ ↑	Positive	2.5115	0.05682
		PS (16:0/16:0) PA (16:0/16:0)	↓ ↓	Negative	14.094	0.47018
Linoleic acid metabolism	1	Phosphatidylcholine	↑	Negative	3.6533	0
Alpha-linolenic acid metabolism	1	Phosphatidylcholine	↑	Negative	3.405	0
Glycosylphosphatidylinositol (GPI)-anchor biosynthesis	1	Phosphatidylethanolamine	↓	Negative	3.0432	0.07576
Glycerolipid metabolism	1	PA(16:0/16:0)	↓	Negative	2.7253	0.0192
Arachidonic acid metabolism	1	Phosphatidylcholine	↑	Negative	2.2011	0

Table 5 Related metabolic pathways and corresponding difference metabolites between stages V and IV of female black rockfish

Pathway	Hits	Metabolites	Trend	Ion mode	-ln(p)	Impact
Glycerophospholipid metabolism	4	Phosphatidylethanolamine Phosphatidylcholine	↓ ↓	Positive	2.5115	0.05682
		PS (16:0/16:0) PA (16:0/16:0)	↓ ↓	Negative	14.094	0.47018
Linoleic acid metabolism	1	Phosphatidylcholine	↓	Negative	3.6533	0
Alpha-linolenic acid metabolism	1	Phosphatidylcholine	↓	Negative	3.405	0
Glycosylphosphatidylinositol (GPI)-anchor biosynthesis	1	Phosphatidylethanolamine	↓	Negative	3.0432	0.07576
Glycerolipid metabolism	1	PA (16:0/16:0)	↓	Negative	2.7253	0.0192
Arachidonic acid metabolism	1	Phosphatidylcholine	↓	Negative	2.2011	0
Linoleic acid metabolism	1	Phosphatidylcholine	↓	Negative	3.6533	0

during the development of the ovary (Huang et al. 2010). All of the above results in an overall decreasing trend in phospholipid levels.

In general, the main nutrient in the maturation process of gonads of black rockfish is PC, which plays a key role in sperm maturation and yolk accumulation. However, the changes in individual lipids do not represent all of the changes in gonadal phospholipid composition because the lipidomics pathways of phospholipids are relatively complex and show interactions between metabolites; moreover, the levels of various phospholipids are closely related to regulatory enzymes. From the gene level, we verified the gonadal response mechanism of black rockfish in the reproductive period.

In glycerophospholipid metabolism, PC is used as the substrate, and *pld1* and *pld2* produce the second messenger PA, which then responds to the cell biological process and is metabolized into lipids with various biological functions. In addition, PA activates the mTOR signaling pathway and plays an important role in cell transcription, translation, and skeletal recombination (Schmelzle and Hall 2000). During the nonbreeding period, *pld* was mainly expressed in the brain, liver, gonads, and other tissues via blood to participate in the process of phospholipid decomposition and signal transduction. During the maturation process, *pld* decreased in the gonad with nutrient accumulation in the ovaries, and the hydrolysis of PC was prevented, which acts as the main component of yolk. On the other hand, as a complex regulatory process, the maturation process is always companied by variations in hormone levels in other tissues under the signal transduction of second messengers such as PA. As a result, the expression level of *pld* in the brain increased continuously.

In contrast, in males, the expression level of *pld* maintained a dynamic balance in the brain, liver, and gonad during nonbreeding period. However, with the maturation of sperm, the expression level of *pld* was significantly increased in the testis. It is possible that spermatids were undergoing meiosis, which leads to the quick dephosphorylation and degradation of PA. DAG, the product of PA, activates PKC to promote glycogen decomposition to provide energy for sperm maturation, while PKC inhibits the stimulation of partial agonists to regulate the expression level of *pld* (Exton 2002).

Under normal physiological conditions, phospholipid transferase specifically transports PS and PE into the membrane, while invertase transports PS and PC out of the membrane (Lin et al. 2014). Therefore, the PC/PE ratio is often used as an index to evaluate membrane stability. In the cell, PC and PE, as substrates, are converted into PS by *ptdss1* and *ptdss2*, respectively (Tomohiro et al. 2009). PS is mainly distributed in the brain and has a significant effect in the central nervous system, which can improve the activity of brain cells (McDaniel et al. 2002). Because gonad maturation is regulated by the neuroendocrine axis, the increase in *ptdss* genes in the brain of female black rockfish may be related to the brain regulation of oocyte development and maturation. The variation in *ptdss* genes in the liver was consistent with the lipidomics results. At the end of the IV period, the expression of PS in the liver decreased significantly, thereby maintaining the levels of amino acids and other energy substances in the liver and providing nutrition for the development of ovaries. When the oocyte undergoes final maturation, phospholipids are used for energy metabolism. Compared with female,

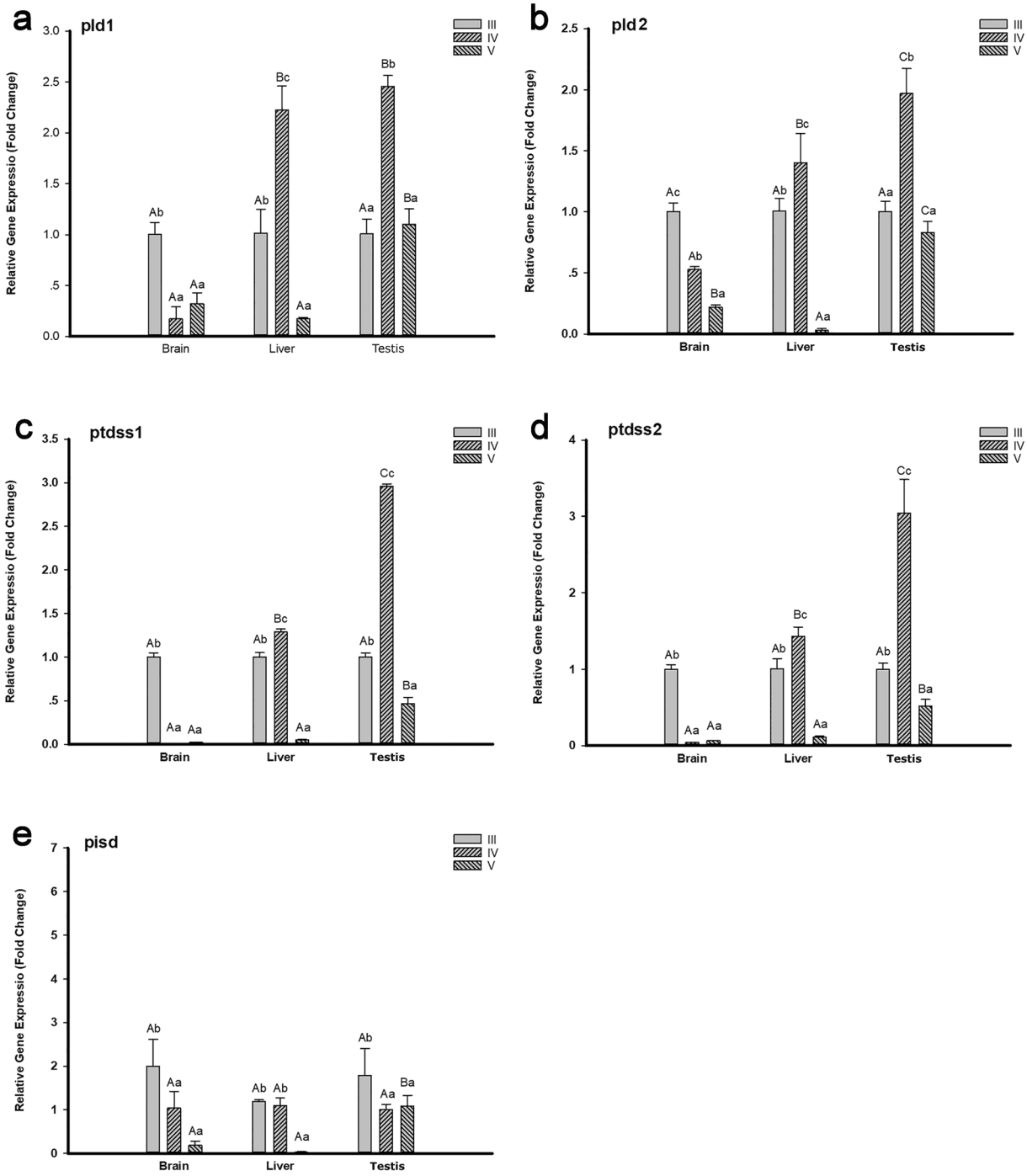

Fig. 8 *pld1*, *pld2*, *ptdss1*, *ptdss2*, and *pld* gene relative expression levels of brain, liver, and testis tissues in different gonadal stages of male black rockfish. Values are given as mean ± SD, $n = 4$. Various letters on top of the column indicated significant differences ($P < 0.05$)

ptdss mRNA expression in the brain of male black rockfish decreased with the maturation of sperm, which may be due to the synthesis of PS, mainly with PE as the substrate in the male brain; as a result, *ptdss1* expression was barely detected. However, to ensure the balance of PC/PE on both sides of the membrane and avoid the eversion of PS, the expression level of *ptdss2* was low at the same time.

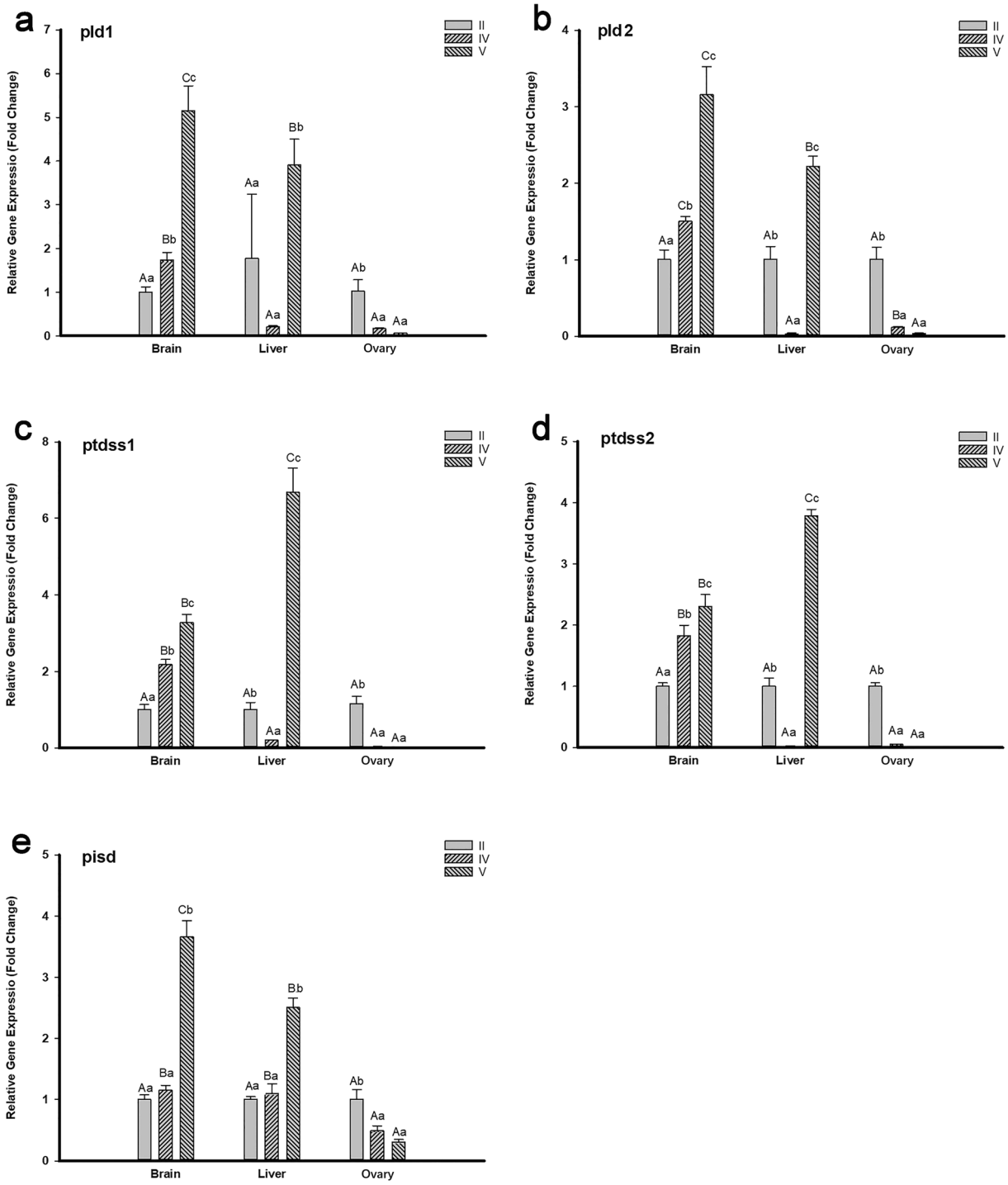

Fig. 9 *pld1*, *pld2*, *ptdss1*, *ptdss2*, and *pld* gene relative expression levels of brain, liver, and ovary tissues in different gonadal stages of female black rockfish. Values are given as mean ± SD, $n = 4$. Various letters on top of the column indicated significant differences ($P < 0.05$)

pisd is mainly expressed in the liver and cerebral cortex (Kevala and Kim 2001). Previous studies showed that almost all mitochondrial PE was synthesized in mitochondria by Pisd and transported out of

mitochondria (Shiao et al. 1995; Steenbergen et al. 2005). The expression of *pisd* decreased in stage IV during spermatozoa maturation, while the PE level increased significantly to supplement the decreased expression of the *pisd* enzyme. However, the decrease in PS concentration and the increase in PE in stage V may be due to the downregulation of *ptdss2* expression to decrease the conversion rate of PE to PS in the testis. Similar trends of *pisd* in the brain and liver were also observed. In stage V, apoptosis starts, and most of PS are valgus as sperm enter the stage of degenerative absorption, and the level of PS in the membrane decreases, thus leading to a decrease in *pisd* expression.

Our present study provides novel insights into the lipidomics profile during gonadal development of an ovoviviparity teleost. In summary, we show that PS, PE, PC, and PA vary during both testis and ovary development. Furthermore, we identified the key enzymes that participate in the metabolism of these lipids. Finally, the expression profiles of these genes were detected. These results described the lipidomics pathways that are important for gonad development in both sexes of ovoviviparity teleost.

Supplementary Information The online version contains supplementary material available at https://doi.org/10.1007/s10695-021-00936-7.

Code availability Not applicable.

Author's contribution WHS, LY, and QX designed the study. SM performed the metabolome and qRT-PCR experiment. LLK, WXJ, ZY, SM, and LJS performed in samples collection. LJS wrote the manuscript, and QX provided manuscript editing and feedback. All authors read and approved the final manuscript.

Funding This study was supported by the National Natural Science Foundation of China (41676126, 41976089) and the National Key R&D Program of China (2018YFD0901204). Our funding agencies did not play a role in the study design, data collection, analysis, interpretation of the data, or preparation of the manuscript.Data AvailabilityThe authors confirm that the data supporting the findings of this study are available within the article and its supplementary materials.

Declarations

Ethical approval All procedures involved in dealing of fish in this study were approved by the Animal Research and Ethics Committees of the Ocean University of China (Permit Number: 20141201) prior to the initiation of the study. The studies did not involve endangered or protected species. And all experiments were performed in accordance with the Guidelines for the Care and Use of Laboratory Animals in China.

Consent to participate Not applicable.

Consent for publication Not applicable.

Conflict of interest The authors declare no competing interests.

References

Aktas M, Wessel M, Hacker S, Klüsener S, Gleichenhagen J, Narberhaus F (2010) Phosphatidylcholine biosynthesis and its significance in bacteria interacting with eukaryotic cells. Eur J Cell Biol 89:888–894

Aloia RC (1983) Membrane fluidity in biology. Cellular Aspects: 293–300

Bergo MO, Gavino BJ, Steenbergen R, Sturbois B, Parlow AF, Sanan DA, Skarnes WC, Vance JE, Young SG (2002) Defining the importance of phosphatidylserine synthase 2 in mice. J Biol Chem 277:47701–47708

Blankenberg FG, Katsikis PD, Tait JF, Davis RE, Naumovski L, Ohtsuki K, Kopiwoda S, Abrams MJ, Darkes M, Robbins RC, Maecker HT, SH W (1998) In vivo detection and imaging of phosphatidylserine expression during programmed cell death. Proc Natl Acad Sci U S A 95:6349–6354

Borkenhagen LF, Kennedy EP, Fielding L (1961) Enzymatic formation and decarboxylation of phosphatidylserine. J Biol Chem 236:28–PC30

Buckland AG, Wilton DC (2000) Anionic phospholipids, interfacial binding and the regulation of cell functions. Biochim Biophys Acta 1483:199–216

Calzada E, Onguka O, Claypool SM (2016) Phosphatidylethanolamine metabolism in health and disease. Int Rev Cell Mol Biol 321:29–88

Castellini C, Cardinali R, Bosco AD, Minelli A, Camici O (2006) Lipid composition of the main fractions of rabbit semen. Theriogenology 65:703–712

Dennis RV (2003) New perspectives on the regulation of intermembrane glycerophospholipid traffic. J Lipid Res 44:441–449

Drokin SI (1993) Phospholipids and fatty acids of phospholipids of sperm from several freshwater and marine species of fish. Comp Biochem Physiol B 104:423–428

English D, Cui Y, Siddiqui RA (1996) Messenger functions of phosphatidic acid. Chem Phys Lipids 80:117–132

Evans RW, Setchell BP (1978) Association of exogenous phospholipids with spermatozoa. J Reprod Fertil 53:357–362

Exton JH (1994) Phosphatidylcholine breakdown and signal transduction. BBA- Lipids and Lipid Metabolism 1212:26–42

Exton JH (2002) Regulation of phospholipase D. FEBS Lett 531: 58–61

Gao TX, Ding K, Song N, Zhang X, Han Z (2017) Comparative analysis of multiple paternity in different populations of viviparous black rockfish, Sebastes schlegelii, a fish with long-term female sperm storage. Mar Biodivers 6:1–8

Geiger O, López-Lara IM, Sohlenkamp C (2013) Phosphatidylcholine biosynthesis and function in bacteria. BBA- Molecular and Cell Biology of Lipids 1831:503–513

Goldfine H (1982) Lipids of prokaryotes–structure and distribution. Curr Top Membr Trans 17:1–43

Hashemi HF, Goodman JM (2015) The life cycle of lipid droplets. Curr Opin Cell Biol 33:119–124

Hinkovska-Galcheva V, Petkova D, Koumanov K (1989) Changes in the phospholipid composition and phospholipid asymmetry of ram sperm plasma membranes after cryopreservation. Cryobiology 26:70–75

Hiratsuka S, Kitagawa T, Matsue Y, Hashidume M, Wada S (2004) Lipid class and fatty acid composition of phospholipids from the gonads of skipjack tuna. Fish Sci 70:903–909

Hu C, Heijden RVD, Wang M, Greef JVD, Hankemeier T, Xu G (2009) Analytical strategies in lipidomics and applications in disease biomarker discovery. J Chromatogr B Anal Technol Biomed Life Sci 877:2836–2846

Huang X, Yin Y, Shi Z, Li W, Zhou H, Lv W (2010) Lipid content and fatty acid composition in wild-caught silver pomfret (Pampus argenteus) broodstocks: effects on gonad development. Aquaculture 310:192–199

Kawaguchi M, Nakagawa M, Noda T, Yoshizaki N, Hiroi J, Nishida M, Iuchi I, Yasumasu S (2010) Hatching enzyme of the ovoviviparous black rockfish Sebastes schlegelii- environmental adaptation of the hatching enzyme and evolutionary aspects of formation of the pseudogene. FEBS J 275: 2884–2898

Kevala JH, Kim HY (2001) Determination of substrate preference in phosphatidylserine decarboxylation by liquid chromatography–electrospray ionization mass spectrometry. Anal Biochem 292:130–138

Küllenberg D, Taylor LA, Schneider M, Massing U (2012) Health effects of dietary phospholipids. Lipids Health Dis 11:1–16

Lee ZW, Kweon SM, Kim BC, Leem SH, Shin I, Kim JH, Ha KS (1998) Phosphatidic acid-induced elevation of intracellular Ca2+ is mediated by RhoA and H2O2 in Rat-2 fibroblasts. J Biol Chem 273:12710–12715

Lin Q, London E, Holowka D (2014) Preparation of artificial plasma membrane mimicking vesicles with lipid asymmetry. PLoS One 9:e87903

Livak KJ, Schmittgen TD (2001) Analysis of relative gene expression data using real-time quantitative PCR and the $2^{-\Delta\Delta CT}$ Method. Methods 25:402–408

Ma LM, Wang WJ, Liu CH, Yu HY, Wang ZG, Wang XB, Qi J, Zhang QQ (2013) Selection of reference genes for reverse transcription quantitative real-time PCR normalization in black rockfish (Sebastes schlegeli). Mar Genomics 11:67–73

Marei WF, Wathes DC, Fouladi-Nashta AA (2012) Differential effects of linoleic and alpha-linolenic fatty acids on spatial and temporal mitochondrial distribution and activity in bovine oocytes. Reprod Fert Develop 24:679–690

McDaniel M, Maier SF, Einstein G (2002) "Brain-specific" nutrients: a memory cure? Psychol Sci Public Interest 3:12–38

Mori H, Nakagawa M, Soyano K, Koya Y (2011) Annual reproductive cycle of black rockfish Sebastes schlegeli in captivity. Fish Sci 69:910–923

Mürke E, Stoll S, Lendeckel U, Reinhold D, Schild L (2016) The mitochondrial phospholipid cardiolipin is involved in the regulation of T-cell proliferation. BBA - Mol Cell Biol L 1861:748–754

Nicolson GL, Ash ME (2017) Membrane lipid replacement for chronic illnesses, aging and cancer using oral glycerolphospholipid formulations with fructooligosaccharides to restore phospholipid function in cellular membranes, organelles, cells and tissues. BBA - Biomembranes 1859: 1704–1724

Paczkowski M, Schoolcraft WB, Krisher RL (2014) Fatty acid metabolism during maturation affects glucose uptake and is essential to oocyte competence. Reproduction 148:429–439

Paulini F, Silva RC, JLJdPRCM L (2014) Ultrastructural changes in oocytes during folliculogenesis in domestic mammals. J Ovarian Res 7:102

Roustaian P, Kamarudin MS, Omar H, Saad CR, Ahmad MH (1999) Changes in fatty acid profile during larval development of freshwater prawn Macrobrachium rosenbergii (de Man). Aquac Res 30:815–824

Rücker-Martin C, Hénaff M, Hatem SN, Delpy E, Mercadier J-J (1999) Early redistribution of plasma membrane phosphatidylserine during apoptosis of adult rat ventricular myocytes in vitro. Basic Res Cardiol 94:171–179

Salze G, Tocher DR, Roy WJ, Robertson DA (2010) Egg quality determinants in cod (Gadus morhua L.): egg performance and lipids in eggs from farmed and wild broodstock. Aquac Res 36:1488–1499

Schmelzle T, Hall MN (2000) TOR, a central controller of cell growth. Cell 103:253–262

Shiao Y, Lupo G, Vance JE (1995) Evidence that phosphatidylserine is imported into mitochondria via a mitochondria-associated membrane and that the majority of mitochondrial phosphatidylethanolamine is derived from decarboxylation of phosphatidylserine. J Biol Chem 270: 11190–11198

Simpson AM, Swan MA, White IG (1986) Action of phosphatidylcholine in protecting ram sperm from cold shock. Mol Reprod Dev 15:43–56

Sohlenkamp C, IM L, Geiger O (2003) Biosynthesis of phosphatidylcholine in bacteria. Prog Lipid Res 42:115–162

Songlin L, Wen W, Xu G, Xuxiong H, Naisong C (2018) Variation of lipids and fatty acids composition in the tissues of wild devil stinger (Inimicus japonicas) during sexual maturation. Aquaculture & Fisheries 3:115–121

Steenbergen R, Nanowski TS, Beigneux A, Kulinski A, Young SG, Vance JE (2005) Disruption of the phosphatidylserine decarboxylase gene in mice causes embryonic lethality and mitochondrial defects. J Biol Chem 280:40032–40040

Stone SJ, Vance JE (1999) Cloning and expression of murine liver phosphatidylserine synthase (PSS)-2: differential regulation of phospholipid metabolism by PSS1 and PSS2. Biochem J 342:57–64

Sturbois-Balcerzak B, Stone SJ, Sreenivas A, Vance JE (2001) Structure and expression of the murine phosphatidylserine synthase-1 gene. J Biol Chem 276:8205–8212

Taneva SG, Lee J, Knowles DG, Tishyadhigama C, Cornell RB (2019) Interdomain communication in the phosphatidylcholine regulatory enzyme, CCTα, relies on a modular αE helix. Journal of Biological Chemistry 294:jbc.RA119.009849

Tocher DR, Bendiksen EÅ, Campbell PJ, Bell JG (2008) The role of phospholipids in nutrition and metabolism of teleost fish. Aquaculture 280:21–34

Tomohiro S, Kawaguti A, Kawabe Y, Kitada S, Kuge O (2009) Purification and characterization of human

phosphatidylserine synthases 1 and 2. Biochem J 418:421–429

Toyomizu M, Hanaoka K, Satake K, Nakagawa H (1977) Effect of storage temperatures on accumulation of glycerylphosphorylcholine and decomposition of phosphatidylcholine in fish muscle during cold storage. Nippon Suisan Gakkaishi 43:1181–1187

Vance JE (2015) Phospholipid synthesis and transport in mammalian cells. Traffic 16:1–18

Vance JE, Tasseva G (2013) Formation and function of phosphatidylserine and phosphatidylethanolamine in mammalian cells. BBA - Molecular and Cell Biology of Lipids 1831:543–554

Warzych E, Pawlak P, Pszczola M, Cieslak A, Madeja ZE, Lechniak D (2017) Interactions of bovine oocytes with follicular elements with respect to lipid metabolism. Anim Sci J 88:1491–1497

Wiegand MD (1996) Composition, accumulation and utilization of yolk lipids in teleost fish. Rev Fish Biol Fish 6:259–286

Wouters R, Molina C, Lavens P, Calderón J (2001) Lipid composition and vitamin content of wild female Litopenaeus vannamei in different stages of sexual maturation. Aquaculture 198:307–323

Zwaal RFA, Schroit AJ (1997) Pathophysiologic implications of membrane phospholipid asymmetry in blood cells. Blood 89:1121–1132